Contribution from the Laboratoire de Chimie Quantique, ER 139 du CNRS, Université Louis Pasteur, 67000 Strasbourg, France

Coordination Mode and Bonding Nature of Carbon Dioxide in d^8 $[Co(alcn)_2(CO_2)]^-$ (alcn = $HNCHCHCHO^-$). An ab Initio MO Study

S. Sakaki*[1] and A. Dedieu

Received December 5, 1986

A theoretical study, based on ab initio MO calculations, has been carried out on a d^8 Co(I)-CO_2 complex, $[Co(alcn)_2(CO_2)]^-$ (alcn = $HNCHCHCHO^-$), which has been examined as a model of the well-known η^1-C-coordinated CO_2 complex M[Co(R-salen)(CO_2)] (R-salen = alkyl- (R-) substituted *N,N'*-ethylenebis(salicylideneaminato); M = alkali-metal cation). The η^1-C coordination mode is calculated to be the most stable among the three possible coordination modes (η^2 side-on, η^1-C coordination, and η^1-O end-on modes), whereas the η^2 side-on and η^1-O end-on modes appear to be unstable. These results are well rationalized in terms of molecular orbital interactions, taking into account the electrostatic interaction between CO_2 and $[Co(alcn)_2]^-$. On the basis of the same criteria, the coordination mode of CO_2 is predicted for various transition-metal complexes. Driving forces for the CO_2 bending and effects of an alkali-metal countercation are also investigated; the CO_2 bending strengthens the charge-transfer interaction from the Co d_{z^2} orbital to the CO_2 π^* orbital and weakens two pairs of four-electron destabilizing interactions, i.e., Co d_{z^2}-CO_2 π and Co $d\pi$-CO_2 $n\pi$ ($n\pi$ = the nonbonding π orbital). The presence of a Li^+ cation greatly enhances the CO_2 coordination through electrostatic interaction between Li^+ and CO_2 and polarization of CO_2 by Li^+.

Introduction

There is much current interest in transition-metal carbon dioxide complexes with the aim of carbon dioxide fixation into organic substances, since coordination to transition-metal ions is one of the most powerful ways of activating inert molecules.[2] Over the last decade, intense efforts have been made to synthesize and characterize transition-metal carbon dioxide complexes. Unfortunately, carbon dioxide very rarely forms stable adducts with transition metals, and only a restricted number of transition-metal carbon dioxide complexes have been isolated and structurally characterized.[3-7] Furthermore, effective catalytic reduction of carbon dioxide to useful organic substances has not been generally successful, except for the case of a few pioneering works.[7c,8-11]

In this light, we need fundamental information concerning bonding nature, stereochemistry, reactivity, and electronic structure of transition-metal carbon dioxide complexes. Such information can be obtained from a theoretical study of transition-metal carbon dioxide complexes. Yet, only a few MO investigations have been reported,[12-14] and the above-mentioned issues have not been fully elucidated. A comprehensive discussion of the coordination mode is still lacking, and factors determining the coordination mode are also ambiguous, although one of the characteristic features of transition-metal carbon dioxide complexes is the presence of several coordination modes, i.e. the η^1-C mode (**1**), the η^2 side-on mode (**2**), and the η^1-O end-on mode (**3**) (Chart I). Some of these modes have been discussed in an ab initio MO study of Ni(P-$H_3)_2(CO_2)$[13] and an EH-MO study of $[Co(NH_3)_4(CO_2)]^+$.[14] However, both studies do not seem sufficient; for example, in the ab initio MO study a detailed discussion of the η^1-C mode was not reported, and in the EH-MO study the electrostatic interaction, which might be important for determining the relative stability of the three coordination modes, is hardly taken into account.

Chart I

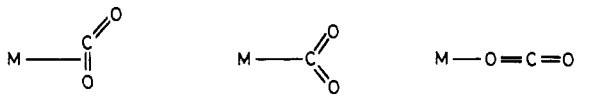

η^2 side on (**1**) η^1-C (**2**) η^1-O end on (**3**)

Hence, the interaction between carbon dioxide and a metal center should be theoretically investigated in more detail, in order to get convincing information about the coordination modes. We present here an ab initio MO study of the η^1-C-coordinated Co(I)-CO_2 complex $[Co(alcn)_2(CO_2)]^-$ (alcn = $HNCHCHCHO^-$), either with or without the Li^+ countercation. This complex is believed to be a realistic model of M[Co(R-salen)(CO_2)] (M = alkali-metal cation; R-salen = alkyl- (R-) substituted *N,N'*-ethylenebis(salicylideneaminato)), which is a well-known η^1-C-coordinated carbon dioxide complex.[4] Our goal is (a) to elucidate why the η^1-C coordination mode is stable but why the other modes are not isolated in the Co(I) complex, (b) to clarify the driving force necessary to distort carbon dioxide from its equilibrium linear structure to the bent one in the Co(I) complex, and (c) to delineate the effect of an alkali-metal countercation on the CO_2 coordination. It is also our intention with this work to summarize the results of MO studies of transition-metal carbon dioxide complexes and to present general rules for predicting the coordination mode by considering the nature of the metal center.

Computational Details

All-electron ab initio MO calculations of $[Co(alcn)_2]^-$, $[Co(alcn)_2(CO_2)]^-$, and $Li[Co(alcn)_2(CO_2)]$ were carried out with two different basis sets by using the IMSPAK[15] and ASTERIX[16] program systems. In a

(1) Present address: Department of Applied Chemistry, Faculty of Engineering, Kumamoto University, Kurokami, Kumamoto, 860 Japan.
(2) For example: Palmer, D. A.; Van Eldik, R. *Chem. Rev.* **1983**, *83*, 651. Darensbourg, D. J.; Kudaroski, R. A. *Adv. Organomet. Chem.* **1983**, *22*, 129.
(3) Aresta, M.; Nobile, C. F.; Albano, V. G.; Forni, E.; Manassero, M. *J. Chem. Soc., Chem. Commun.* **1975**, 636.
(4) (a) Fachinetti, G.; Floriani, C.; Zanazzi, P. F. *J. Am. Chem. Soc.* **1978**, *100*, 7405. (b) Gambarotta, S.; Arena, F.; Floriani, C.; Zanazzi, P. F. *J. Am. Chem. Soc.* **1982**, *104*, 5082.
(5) Bristow, G. S.; Hitchcock, P. B.; Lappert, M. F. *J. Chem. Soc., Chem. Commun.* **1981**, 1145.
(6) Calabrese, J. C.; Herskobitz, T.; Kinney, J. B. *J. Am. Chem. Soc.* **1983**, *105*, 5914.
(7) (a) Alvarez, R.; Carmona, E.; Poveda, M. L.; Sánchez-Delgado, R. *J. Am. Chem. Soc.* **1984**, *106*, 2731. (b) Alvarez, R.; Carmona, E.; Marín, J. M.; Poveda, M. L.; Gutiérrez-Puebla, E.; Monge, A. *J. Am. Chem. Soc.* **1986**, *108*, 2286. (c) Albarez, R.; Carmona, E.; Cole-Hamilton, D. J.; Galindo, A.; Gutiérrez-Puebla, E.; Monge, A.; Poveda, M. L.; Ruiz, C. *J. Am. Chem. Soc.* **1985**, *107*, 5529.
(8) Bodnar, T.; Coman, E.; Menard, K.; Cutler, A. *Inorg. Chem.* **1982**, *21*, 1275.
(9) (a) Fisher, B.; Eisenberg, R. *J. Am. Chem. Soc.* **1980**, *102*, 7361. (b) Lieber, C. M.; Lewis, N. S. *J. Am. Chem. Soc.* **1984**, *106*, 5033.
(10) Darensbourg, D. J.; Ovalles, C. *J. Am. Chem. Soc.* **1984**, *106*, 3750.
(11) (a) Takeda, N.; Inoue, S. *Bull. Chem. Soc. Jpn.* **1978**, *51*, 3564. (b) Aida, T.; Inoue, S. *J. Am. Chem. Soc.* **1983**, *105*, 1304. (c) Kojima, F.; Aida, T.; Inoue, S. *J. Am. Chem. Soc.* **1986**, *108*, 391.
(12) (a) Sakaki, S.; Kudou, N.; Ohyoshi, A. *Inorg. Chem.* **1977**, *16*, 202. (b) Demoulin, D.; Pullmann, A. *Theoret. Chim. Acta* **1978**, *49*, 161. (c) Ozin, G. A.; Huber, H.; McIntosh, D. *Inorg. Chem.* **1978**, *17*, 1472.
(13) Sakaki, S.; Kitaura, K.; Morokuma, K. *Inorg. Chem.* **1982**, *21*, 760.
(14) Mealli, C.; Hoffmann, R.; Stockis, A. *Inorg. Chem.* **1984**, *23*, 56.
(15) Morokuma, K.; Kato, S.; Kitaura, K.; Ohmine, I.; Sakai, S.; Obara, S. Program 0372, IMS Computer Program Library, The Institute for Molecular Science, 1980. This program was used after minor modification by S.S.
(16) Bénard, M.; Dedieu, A.; Demuynck, J.; Rohmer, M. M.; Strich, A.; Veillard, A., unpublished work.

0020-1669/87/1326-3278$01.50/0

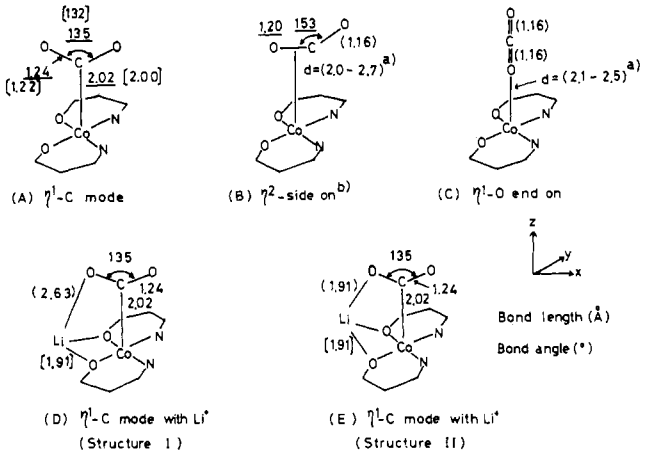

Figure 1. Geometry of Co(I)–CO_2 complexes examined here: underline, optimized value; [ ], experimental value; ( ), assumed value. (a) No local minimum was found in this region examined. (b) The geometry of the CO_2 part was optimized at d = 2.0 Å.

smaller basis (SB) set, a (12s 7p 5d) primitive set contracted to [5s 3p 3d],[17] the usual 4-31G, and the 31G basis sets[18] were used for the cobalt, the first-row, and the hydrogen atoms, respectively. Geometry optimization and preliminary investigation of Co(I)–CO_2 complexes were carried out with this basis set. A larger basis (LB) set was employed for an energetic comparison of various structures and a discussion of the bonding nature. In the LB set, a (14s 9p 5d) primitive set was contracted to [6s 4p 3d] for cobalt.[19] Standard (9s 5p) and (4s) sets[20] were contracted to [3s 2p] and [2s] for the first-row and hydrogen atoms, respectively. For the lithium atom, a (9s 4p) primitive set was constracted to [3s 2p].[21]

A closed-shell singlet state was assumed for $[Co(alcn)_2]^-$, $[Co(alcn)_2(CO_2)]^-$, and $Li[Co(alcn)_2(CO_2)]$, as described in our preliminary work,[22] since diamagnetism has been experimentally reported in Na[Co(R-salen)],[4b] Na[Co(R-salen)(CO_2)], and Na[Co(R-salen)(py)(CO_2)][23] (py = pyridine).

The structures of Co(I)–CO_2 complexes examined here are displayed in Figure 1. Some geometrical parameters important for the carbon dioxide coordination were optimized, while the remaining geometrical parameters of the $Co(alcn)_2$ moiety were taken from appropriate references and fixed during optimization. For instance, the geometries of the CoN_2O_2 core and the alcn ligand were taken from the experimental structures of K[Co(Pr-salen)(CO_2)][4b] and $[Co(salen)_2]$[24] (salen = bis(salicylaldehyde) ethylenediimine), respectively, assuming a planar structure of the $Co(alcn)_2$ part. In the η^1-C mode, the Co–C and C–O distances and the OCO angles were optimized independently, assuming a *Cs* symmetry[4b] and equal C–O bond distances (Figure 1A).[25a] In the η^2 side-on mode, the coordinated C=O bond was placed on the *xz* plane perpendicularly to the *z* axis. The coordinated C=O bond length and the OCO angle of carbon dioxide were optimized at R = 2.0 and 2.5 Å (see Figure 1B for R), while the other C=O bond length was kept at 1.160 Å (the experimental value of carbon dioxide).[25b] In the η^1-O end-on mode, the CO_2 ligand was placed on the *z* axis perpendicularly to the $Co(alcn)_2$ plane, assuming the two C=O bond distances to be 1.160 Å and varying only the Co–O distance. Although the examination of this mode seems rather brief, it was found certainly that this mode is unlikely even in a local minimum, as will be described later.

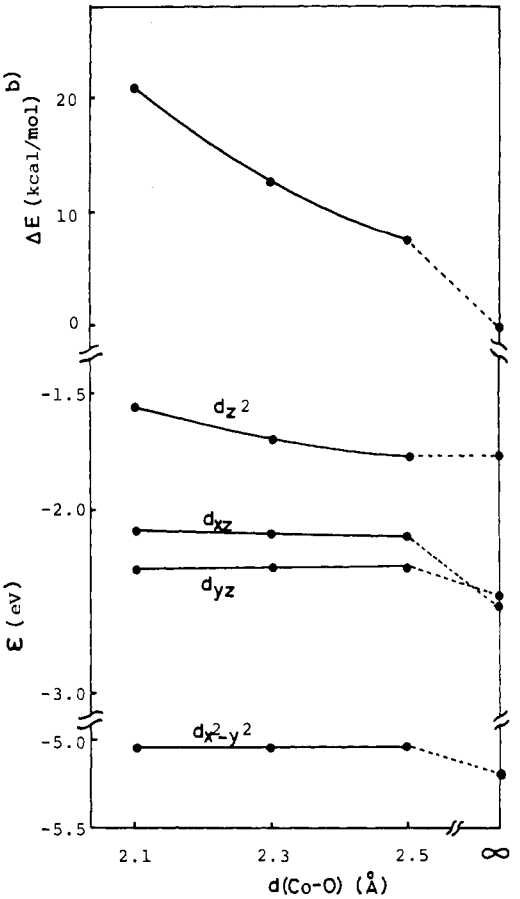

Figure 2. Variation of total energy and energy level of d orbitals near the HOMO as a function of the R(Co–O) distance in the η^1-C end-on mode (see note a). (a) The small basis set is used. (b) $\Delta E = E_t\{[Co(alcn)_2(CO_2)]^-\} - E_t\{[Co(alcn)_2]^-\} - E_t(CO_2)$.

To investigate the nature of the bonding, the energy decomposition analysis (EDA), proposed by Morokuma et al.,[26] was applied here. Since this EDA method has been reported elsewhere,[26] only its outline is given here. The total complex, $[Co(alcn)_2(CO_2)]^-$, is considered to consist of two fragments, the $[Co(alcn)_2]^-$ part and the CO_2 ligand. The binding energy (BE), the deformation energy (DEF), and the interaction energy (INT) are defined, as follows:

$$BE = E_t\{[Co(alcn)_2(CO_2)]^-\}_{opt} - E_t\{[Co(alcn)_2]^-\} - E_t(CO_2)_{eq} = DEF + INT \quad (1)$$

$$DEF = E_t(CO_2)_{dist} - E_t(CO_2)_{eq} \quad (2)$$

$$INT = E_t\{[Co(alcn)_2(CO_2)]^-\}_{opt} - E_t\{[Co(alcn)_2]^-\} - E_t(CO_2)_{dist} \quad (3)$$

The subscripts "eq" and "dist" denote the equilibrium structure and distorted structure, respectively (note that CO_2 is distorted in the Co(I)–CO_2 complex). INT is then divided into several terms

$$INT = ES + EX + FCTPLX + BCTPLX + R \quad (4)$$

i.e. electrostatic (ES), exchange repulsion (EX), forward charge transfer from CO_2 to $[Co(alcn)_2]^-$ (FCTPLX), back charge transfer from [Co-

(17) The original set of (12s 6p 4d) presented by Roos–Veillard–Vinot was augmented by a primitive p function (exponent ζ = 0.118 259) and a diffuse d primitive function with an exponent proposed by Hay: Roos, B.; Veillard, A.; Vinot, G. *Theoret. Chim. Acta* **1971**, *20*, 1. Hay, P. J. *J. Chem. Phys.* **1977**, *66*, 4377.
(18) Ditchfield, R.; Hehre, W. J.; Pople, J. A. *J. Chem. Phys.* **1971**, *54*, 724.
(19) Hyla-Kryspin, I.; Demuynck, J.; Strich, A.; Bénard, M. *J. Chem. Phys.* **1981**, *75*, 3954. The original (13s 7p 5d) set was modified by adding an s primitive (ζ = 0.3572), two p primitives (ζ = 0.2728, 0.0886), and a d primitive (ζ = 0.1173), where these exponents were estimated from the even-tempered criterion.
(20) Huzinaga, S. "Approximate Wavefunction", Technical Report, University of Alberta, 1971.
(21) Primitives for the s function were taken from ref 20, but primitives for the p function were from the work of: Dunning, T. H.; Hay, P. J. In *Method of Electronic Structure Theory*; Schaeffer, H. F., Ed.; Plenum: New York, 1977; p. 23.
(22) Sakaki, S.; Dedieu, A. *J. Organomet. Chem.* **1986**, *314*, C63.
(23) Floriani, C.; Fachinetti, G. *J. Chem. Soc., Chem. Commun.* **1974**, 615.
(24) Schaefer, W. P.; Marsh, R. E. *Acta Crystallogr., Sect. B: Struct. Crystallogr. Cryst. Chem.* **1969**, *B25*, 1675.
(25) (a) A rotation of CO_2 around the Co–C bond was not examined here, considering the rather large size of $[Co(alcn)_2(CO_2)]^-$. The orientation of the CO_2 ligand was assumed to be the same as that in K[Co(R-salen)(CO_2)].[4b] (b) The length of the C=O bond was optimized to be 1.158 Å with the 4-31G set, which is very close to the experimental value. Sutton, E., Ed. *Tables of Interatomic Distances and Configurations in Molecules and Ions*; Special Publication No. 18; The Chemical Society: London, 1965.
(26) (a) Morokuma, K. *Acc. Chem. Res.* **1977**, *10*, 294. (b) Kitaura, K.; Morokuma, K. *Int. J. Quantum. Chem.* **1976**, *10*, 325. (c) Kitaura, K.; Sakaki, S.; Morokuma, K. *Inorg. Chem.* **1981**, *20*, 2292.

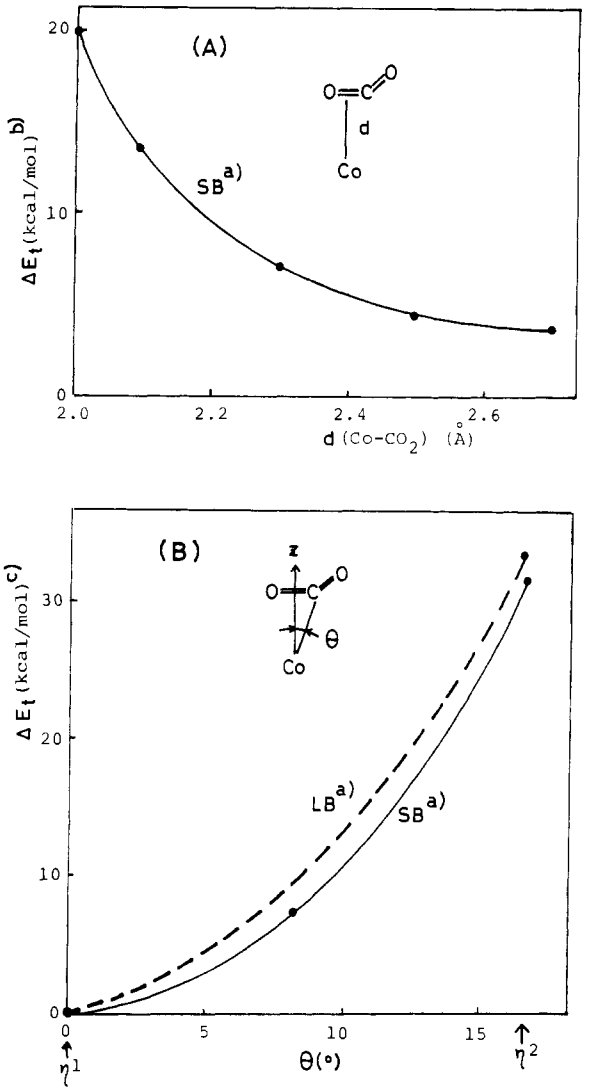

Figure 3. Energy changes along the dissociation path of the CO_2 ligand in the η^2 side-on $[Co(alcn)_2(CO_2)]$ (A) and along the linear transit between the η^1-C mode and the η^2 side-on mode of $[Co(alcn)_2(CO_2)]$ (B). (a) SB = small basis set. LB = larger basis set. See the text (computational details) for SB and LB. (b) The zero of energy for the separate molecules. (c) Zero of energy refers to the η^1-C mode.

$(alcn)_2]^-$ to CO_2 (BCTPLX), and a higher order remaining term (R).[27]

Results and Discussion

Preliminary Investigation of Three Coordination Modes. The optimized structure of the η^1-C mode agrees well with the experimental structure, as shown in Figure 1A. The binding energy of CO_2 in this coordination mode is calculated to be 6.2 kcal/mol by using the LB set.[28a] This value seems rather small for a usual

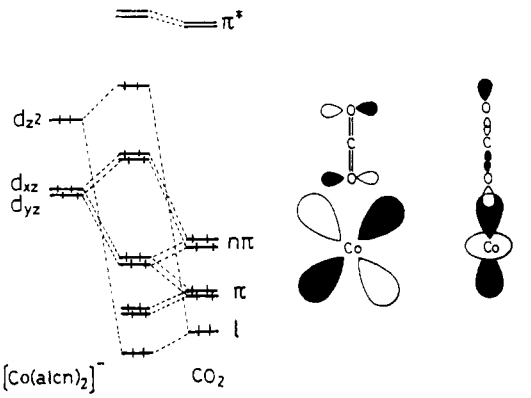

Figure 4. Schematic orbital correlation diagram and the important four-electron destabilizing interactions for the η^1-O end-on mode.

Chart II

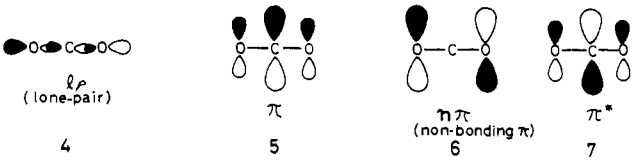

coordination bond. The presence of the Li^+ cation, however, leads to a greater value of ca. 20 kcal/mol (in the LB set calculation).[28b] Thus, it is reasonably concluded that the η^1-C mode is a stable coordination mode and that a Li^+ countercation plays an important role in stabilizing this complex.

The potential energy curve of the η^1-O end-on mode, computed with the SB set, is shown as a function of the distance R between cobalt and oxygen atoms in Figure 2 (see Figure 1C for the definition of R). This curve is apparently repulsive in the range of R = 2.1–2.5 Å, although the SB set tends to overestimate the binding energy. The lengthening of the C=O bond was examined, in order to consider the weakening of the C=O bond upon coordination. Such calculations, however, resulted in further destabilization by ca. 4 and 6 kcal/mol for the lengthening (0.05 Å) of one and two C=O bonds, respectively. We cannot rule out the possibility that some binding energy would be found at an R distance longer than 2.5 Å. But, the interaction between cobalt and carbon dioxide would be very weak for such a long distance and would not correspond to a normal coordination bond. Thus, the η^1-O end-on mode appears to be unlikely in the Co(I) complex, which will be supported later by an orbital interaction diagram.

The potential curve for the η^2 side-on mode is repulsive (see Figure 3A).[31a] The fact that the η^2 mode is less stable than the η^1-C mode is also well exemplified by the conversion to the η^1-C mode from the η^2 mode in which the geometry change was

(27) Carbon dioxide has the Lewis acidic center on the carbon atom and the Lewis basic center on the oxygen atom. In the η^1-C mode, the acidic center interacts with the cobalt of $[Co(alcn)_2]^-$. In this light, the forward charge transfer might be defined as the charge transfer from $[Co(alcn)_2]^-$ to CO_2 strictly speaking. However, the usual definitions of FCTPLX and BCTPLX are used to avoid the confusion with the general concept that the coordinate bond is mainly formed by the charge transfer from ligand to metal.

(28) (a) An MO calculation with the SB set yields a binding energy of 13.6 kcal/mol. In this calculation, the basis set superposition error (BSSE) of the η^1-C mode was estimated to be 14.5 kcal/mol with the ghost orbital (GO) method[29] and 4.2 kcal/mol with the ghost virtual orbital (GVO) method.[30] The true value of BSSE would lie between these two values, since the GO method overestimates the BSSE. A small binding energy is, therefore, expected for this mode. (b) The BSSE value for the LB set should be smaller than the value for the SB set. The value of 20.0 kcal/mol for the binding energy would not be significantly decreased after correction of the BSSE.

(29) Boys, S. F.; Bernardi, F. *Mol. Phys.* **1970**, *19*, 553. Ostlund, N. S.; Merrifield, D. L. *Chem. Phys. Lett.* **1976**, *39*, 612.

(30) This idea has been proposed in the following papers: Petterson, L.; Wahlgren, U. *Chem. Phys.* **1982**, *69*, 185. Bagus, P. S.; Herman, K.; Bauschlicher, C. W. *J. Chem. Phys.* **1984**, *80*, 4378; **1984**, *81*, 1966. Bauschlicher, C. W.; Bagus, P. S. *J. Chem. Phys.* **1984**, *81*, 5889.

(31) (a) The reoptimization of the CO_2 part at R = 2.5 Å resulted in a very small binding energy of 2 kcal/mol (the SB set calculation). The BSSE value was, however, estimated to lie between 6.8 and 2.4 kcal/mol, which were calculated by the GO and GVO methods,[29,30] respectively. Even the smaller value of BSSE cannot lead to the binding energy for the CO_2 coordination after correction of the BSSE. (b) In the η^2 mode, the distance R was taken to be 2.02 Å (the same distance as that of the η^1-C mode) and the geometry of the CO_2 ligand was assumed to be the same as the optimized one at R = 2.0 Å (differences in the structure and energy between R = 2.0 Å and R = 2.02 Å are not expected to be large). Both the geometry change modeled by a linear transit and the assumed geometry of the η^2 mode seem rather arbitrary. In this light, the conversion to the η^1-C from the η^2 mode must be examined in more detail, in future. However, it appears to reasonably conclude that the η^2 mode is less stable than the η^1-C mode, since any effective stabilization was not found in a normal coordinating distance, as described above.

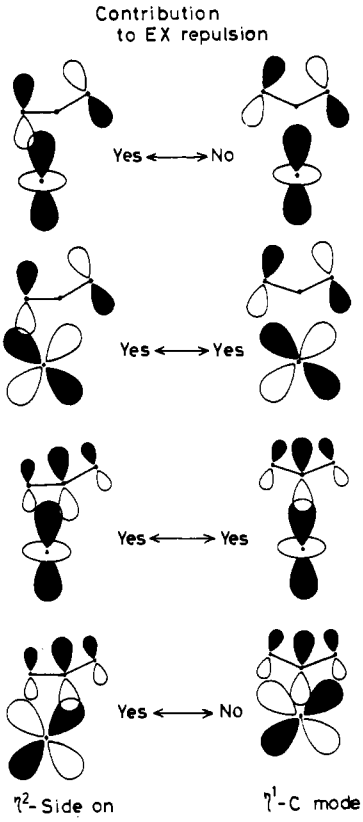

Figure 5. Four-electron destabilizing interactions in the η^1-C mode and η^2 side-on mode.

modeled by a linear transit between these two limiting structures.[31b] The total energy given in Figure 3B shows a continuous decrease on going to the η^1-C mode from the η^2 mode, again suggesting that the η^2 side-on mode does not even remain in a local minimum and is less stable than the η^1-C mode.

From these results, we can draw a reasonable conclusion that the η^1-C mode is the only stable coordination mode in the d^8 $[Co(alcn)_2(CO_2)]^-$ complex.

Why Is the η^1-O End-On Mode Unstable? Before starting a discussion of the three coordination modes, it is instructive to briefly examine important orbitals of carbon dioxide and $[Co(alcn)_2]^-$. In the CO_2 ligand (Chart II) the O-end lone pair (**4**), the π (**5**), the nonbonding $n\pi$ (**6**), and the π^* (**7**) orbitals are important for interaction with the transition metal, of which the first three are doubly occupied, the $n\pi$ is the HOMO, and the π^* orbital is the LUMO. In the η^1-C and η^2 side-on modes, the π, $n\pi$, and π^* orbitals are classified into two types, those belonging to the plane consisting of Co and CO_2 and the others being perpendicular to this plane. The former are expected to play a key role in the interaction between Co and CO_2, as will be discussed later, and are denoted by $\pi_\parallel$, $n\pi_\parallel$, and $\pi^*_\parallel$. The latter are labeled $\pi_\perp$, $n\pi_\perp$, and $\pi^*_\perp$. $[Co(alcn)_2]^-$ has a HOMO, mainly composed of the Co d_{z^2} orbital, at a rather high energy level, −2.36 eV (the LB set calculation). The Co d_{xz} and d_{yz} orbitals lie lower in energy than the HOMO by ca. 0.6 eV. The empty Co 4s and $4p_z$ orbitals, which might be important for the charge-transfer interaction from CO_2 to Co, are found remarkably high in energy above some π^* orbitals of the alcn ligand, suggesting a very weak Lewis acidity for the $[Co(alcn)_2]^-$ system.

From symmetry considerations, the η^1-O end-on mode is expected to involve several σ-type interactions between the lone pair (*lp*) of CO_2 and Co $3d_{z^2}$, 4s, and $4p_z$ orbitals and also π-type interactions between CO_2 π, $n\pi$, and π^* and Co d_π orbitals. Stabilizing interactions arise from the CO_2 *lp*–Co 4s, CO_2 *lp*–Co $4p_z$, and CO_2 π^*–Co d_π pairs, whereas destabilizing interactions arise from the CO_2 *lp*–Co d_{z^2}, CO_2 π–Co d_π, and CO_2 $n\pi$–Co d_π pairs. Both the d_π and d_{z^2} orbitals of cobalt are calculated to be raised in energy by the coordination of CO_2 (see the lower part of Figure 2). Also, CO_2 approaching Co hardly stabilizes the lone pair (*lp*) and $n\pi$ orbitals.[32] Furthermore, the antibonding interactions are found in the Co d_π and d_σ orbitals, as shown in the right half of Figure 4. These results, suggesting that the destabilizing interactions are predominant, are well explained by a schematic picture of the orbital interaction diagram sketched in Figure 4. A characteristic of this diagram is two pairs of four-electron destablizing interactions, one between the Co d_{z^2} orbital and the lone pair of CO_2 and the other between the Co d_π orbital and the $n\pi$ orbital of CO_2. Such an unfavorable situation arises from the presence of high-lying occupied d_{z^2} and d_π orbitals and the absence of a good accepting orbital in $[Co(alcn)_2]^-$. From these results it is concluded that the η^1-O end-on coordination is repulsive owing to four-electron destabilizing interactions.

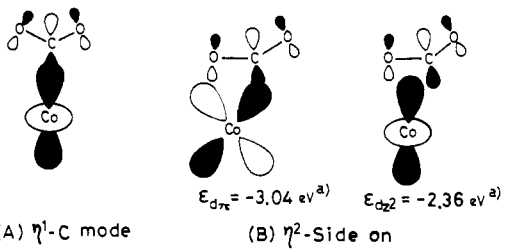

Figure 6. Important charge-transfer interactions in the η^1-C mode and η^2 side-on mode. (a) Orbital energy in $[Co(alcn)_2]^-$. The LB set is used.

Table I. Changes in Electron Population Caused by the Coordination of Carbon Dioxide[a] and Energy Decomposition Analysis of the Interaction between CO_2 and $[Co(alcn)_2]^-$ (kcal/mol)

		η^1-C mode	
	η^2 side on[b]	bent CO_2[c]	linear CO_2[d]
	Electron Populations		
Co	−0.18	−0.40	−0.24
s	+0.04	+0.09	+0.04
p	+0.01	−0.07	−0.10
d	−0.23	−0.43	−0.17
d_{z^2}	−0.07	−0.63	−0.24
d_{xz}	−0.19	0.08	0.04
CO_2	+0.28	+0.71	+0.31
	Energies		
BE	27.0	−6.2	54.8
DEF	16.0	49.2	13.1
INT	11.0	−55.4	41.5
ES	−85.2	−67.9	−83.7
EX	147.6	103.8	170.2
FCTPLX	−14.9	−12.1	−10.8
BCTPLX	−34.1	−53.0	−29.1
R	−2.4	−26.2	−5.1

[a] The LB set is used. [b] This structure is the same as that of η^2 side on given in Figure 1B. [c] The optimized geometry. [d] Only the OCO angle is changed to 180° from the optimized structure.

Comparison of the η^1-C Mode with the η^2 Side-On Mode. Now, let us investigate why only the η^1-C mode is stable and why the η^2 side-on mode does not even remain in a local minimum. In the comparison of the η^1-C mode with the η^2 side-on mode, the four-electron destabilizing interactions will be examined first. As schematically shown in Figure 5, the η^2 side-on mode involves four pairs of four-electron destabilizing interations, i.e. Co d_{z^2}–CO_2 $n\pi_\parallel$, Co d_{z^2}–CO_2 $\pi_\parallel$, Co d_{xz}–CO_2 $n\pi_\parallel$, and Co d_{xz}–CO_2 $\pi_\parallel$. In the η^1-C mode, on the other hand, two of them, the Co d_{z^2}–CO_2 $n\pi_\parallel$ and Co d_{xz}–CO_2 $\pi_\parallel$ pairs, cannot cause a four-electron destabilizing interaction because of their symmetry properties (note that the orbitals belonging to the same symmetry can contribute to the orbital interaction). Consequently, the η^1-C mode suffers less from the four-electron destabilization than the η^2 side-on mode. This result is also corroborated by the energy decomposition

(32) $\varepsilon_{n\pi}$ = −10.88 eV at R_{Co-O} = 2.5 Å and −10.78 eV at R_{Co-O} = 2.1 Å, ε_{lp} = −16.35 eV at R_{Co-O} = 2.5 Å and −16.44 eV at R_{Co-O} = 2.1 Å (the SB set calculation).

Chart III

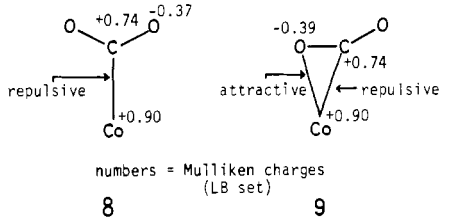

8 9

analysis; as compiled in Table I, the EX repulsion, which includes the four-electron destabilizing interaction as a main contributor, is larger in the η^2 side-on mode than in the η^1-C mode.

In addition to the above-mentioned preferable situation, the η^1-C mode receives remarkably large stabilization from an interaction between the Co d_{z^2} and CO_2 $\pi^*_{\parallel}$ orbitals (see Figure 6). This interaction significantly decreases the electron population of the Co d_{z^2} orbital and substantially increases the electron population of CO_2 upon the CO_2 coordination, as shown in Table I. The η^2 side-on mode also experiences similar charge-transfer interactions, one between the Co d_{z^2} and CO_2 $\pi^*_{\parallel}$ orbitals and another between the Co d_π and CO_2 $\pi^*_{\parallel}$ orbitals. They are rather weak, however; the Co d_{z^2} orbital cannot overlap well with the $\pi^*_{\parallel}$ orbital of CO_2, since the positive overlap between the Co d_{z^2} and carbon p_π orbitals is significantly decreased by the negative overlap between the Co d_{z^2} and oxygen p_π orbitals, as shown in Figure 6B. The Co d_{xz} orbital cannot cause a strong charge-transfer interaction between Co and CO_2 in spite of its good overlap with the $\pi^*_{\parallel}$ orbital of CO_2, since this orbital lies lower in energy than the Co d_{z^2} orbital (see Figure 6B for the energy levels of these d orbitals). Reflecting the weakness of these interactions, the η^2 coordination of CO_2 leads to a smaller decrease in the Co atomic population and a smaller increase in the electron population of CO_2 than the η^1-C coordination. This result is also supported by the energy decomposition analysis. The BCTPLX term includes a charge-transfer interaction between Co and CO_2 as a main contributor. This term offers larger stabilization in the η^1-C mode than in the η^2 side-on mode (see Table I), indicating that the η^1-C mode can cause a stronger charge transfer from Co to CO_2 than the η^2 side-on mode.

The electrostatic interaction, on the other hand, disfavors the η^1-C mode relative to the η^2 side-on mode. The energy decomposition analysis clearly indicates that the η^1-C mode receives smaller stabilization from the ES term than the η^2 side-on mode (see Table I). This result can be easily understood by considering the following electron distribution of the interacting species. The carbon atom is positively charged (+0.73 e Mulliken charge), but the oxygen atom is negatively charged (–0.37 e) in carbon dioxide (distorted stucture). The cobalt atom is positively charged (+0.90 e), in spite of a negative whole charge of $[Co(alcn)_2]^-$. In the η^1-C mode, the carbon atom is placed near the cobalt atom, as shown in Chart III (**8**), yielding an electrostatic repulsion between them. In the η^2 side-on mode, however, the electrostatic repulsion between cobalt and carbon atoms is compensated, to some extent, by the electrostatic attraction between cobalt and oxygen atoms, because both the carbon and the oxygen atoms interact with the cobalt atom (see **9** of Chart III).

In conclusion, the η^1-C mode is stable due to the strong charge-transfer interaction between Co and CO_2 and the weak four-electron destablizing interaction, in spite of the unfavorable situation found in the electrostatic interaction. The η^2 side-on mode is, on the other hand, unstable in $[Co(alcn)_2(CO_2)]^-$, because the strong four-electron destabilizing interaction cannot be overwhelmed by the weak charge-transfer interaction and rather strong electrostatic interaction.

The above discussion and results of a previous study[13] of $Ni(PH_3)_2(CO_2)$ provide us with useful rules to predict the coordination mode of CO_2 in transition-metal complexes. When the metal part has a d_{z^2} orbital as the HOMO, the η^1-C mode can yield a stronger charge-transfer interaction and suffers less from the four-electron destabilizing interaction than the η^2 side-on mode. As a result, the η^1-C mode is more stable than the η^2 side-on mode.

Chart IV

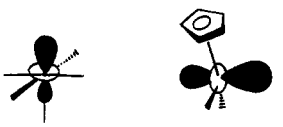

10 11

Table II. Effect of the Coexisting Li^+ Cation on the CO_2 Coordination to $[Co(alcn)_2(CO_2)]^-$[a]

	Mulliken population			
	$Li[Co(alcn)_2]$		$Li[Co(alcn)_2(CO_2)]$	
	I	II	I	II
Co	25.88	25.90	25.47	25.50
d_{z^2}	1.84	1.83	1.24	1.14
CO_2			22.63	22.68
C			5.48	5.46
O_1			8.60	8.68
O_2			8.55	8.54
Li	2.23	2.26	2.25	2.26

[a] The LB set is used. See Figure 1D,E for structures I and II.

From the point of view of the electrostatic interaction, the η^1-C mode is inferior to the η^2 side-on mode, if the central metal is positively charged. In this light, the most desired situation for this mode is the presence of the HOMO mainly composed of a d_σ orbital and a low oxidation state of the metal. $[Co(R\text{-}salen)(CO_2)]^-$[4] and $[RhCl(diars)_2(CO_2)]$,[6] which are well-known as η^1-C-coordinated CO_2 complexes, satisfy these conditions, because both have a d^8-electron configuration of low oxidation state (+1) and their HOMO is mainly composed of the d_{z^2} orbital (see **10** of Chart IV). Consideration of these factors also supports the η^1-C mode inferred for $[IrCl_2L_3(CO_2)]^-$ and $[Fe(\eta\text{-}C_5H_5)(CO)_2(CO_2)]^-$,[33,34] because the $[IrCl_2L_3]^-$ and $[Fe(\eta\text{-}C_5H_5)(CO)_2]^-$ fragments have a d_σ type orbital as the HOMO (see **10** and **11**, respectively, in Chart IV).

When the metal part has a HOMO mainly composed of a d_π orbital like $Ni(PR_3)_2L$ (L = η^2-ligand such as olefin, acetylene, CO_2, CS_2 etc.), the η^2 side-on mode is considerably stabilized by the π-type back-donative interaction.[13] However, if the metal has a doubly occupied d_σ orbital, a four-electron destabilizing interaction arises from the overlap of the d_σ orbital with the π and $n\pi$ orbitals of CO_2. Thus, the best situation for this mode is the presence of a d_π orbital as the HOMO and an empty d_σ orbital pointing to the CO_2 ligand. This situation is found in $[Nb(\eta\text{-}C_5H_4Me)_2(CH_2SiMe_3)(CO_2)]$.[5] The HOMO of the $[Nb(\eta\text{-}C_5H_4Me)_2(CH_2SiMe_3)]$ fragment is a d_π type orbital, whereas the d_σ orbital is empty.[35] $Mo(PR_3)_4(CO_2)_2$ also satisfies these two conditions, which seems an important reason that this complex is very stable in spite of coordination of two carbon dioxide molecules.[7] Unfortunately, $Ni(PR_3)_2(CO_2)$ has both doubly occupied d_π and d_σ orbitals pointing to the CO_2 ligand. Probably, this is one of the reasons that the η^2 side-on structure of the complex deviates, to some extent, toward the η^1-C structure[3] (note that the Ni–C distance is shorter than the Ni–O distance by 0.15 Å).

Bending of the η^1-C-Coordinated Carbon Dioxide. In all of the transition-metal carbon dioxide complexes whose structures have been verified experimentally,[4b] the carbon dioxide is significantly bent from its equilibrium linear structure. This is one of the characteristic features of CO_2 coordination.

In $[Co(alcn)_2(CO_2)]^-$, the linear structure of CO_2 does not yield

(33) (a) Evans, G. O.; Walter, W. F.; Mills, D. R.; Streit, C. A. *J. Organomet. Chem.* **1978**, *144*, C34. (b) Grice, N.; Kao, S. C.; Pettit, R. *J. Am. Chem. Soc.* **1979**, *101*, 1627. (c) Lee, G. R.; Cooper, N. J. *Organometallics* **1985**, *4*, 794.
(34) Bowman, K.; Deening, A. J.; Proud, G. L. *J. Chem. Soc., Dalton Trans.* **1985**, 857.
(35) Tatsumi, K.; Nakamura, A.; Hofmann, P.; Stauffert, P.; Hoffmann, R. *J. Am. Chem. Soc.* **1985**, *107*, 4358.

Table III. Energy Decomposition Analysis of the Interaction between Li^+ and CO_2[a] (kcal/mol)

INT	ES	EX	PL(CO_2)	CT($Li \rightarrow CO_2$)	PL(Li)	CT($CO_2 \rightarrow Li$)	R
−10.3	−8.5	9.9	−11.5	0	0	−1.8	+1.6

[a] The LB is used. The structure of CO_2 is taken to be the same as in $[Co(alcn)_2(CO_2)]^-$.

any stabilization upon CO_2 coordination,[36a] as shown in Table I, while coordination of the bent CO_2 offers moderate stabilization. This means that the bending of CO_2 is essential for the formation of a stable Co(I)–CO_2 complex. The CO_2 bending significantly increases the electron population of CO_2 but remarkably decreases the electron population of the Co d_{z^2} orbital (see Table I). Such electron redistribution suggests that the bending of CO_2 greatly enhances the charge transfer from the Co d_{z^2} orbital to CO_2.[36c] This conclusion is also supported by an energy decomposition analysis, as follows. The BCTPLX term, which includes the charge transfer from Co to CO_2 as a main contributor, yields much larger stabilization in the bent structure than in the linear one. The enhancement of this interaction by the bending is easily explained in terms of the $\pi^*_{\parallel}$ orbital of CO_2. This orbital energy is greatly stabilized by the bending of CO_2; for example, it lies at 3.0 eV in the linear structure but lowers to −0.5 eV in the bent one. Such energy lowering of the $\pi^*_{\parallel}$ orbital yields a strong charge-transfer interaction between Co d_{z^2} and CO_2 $\pi^*_{\parallel}$.

Besides the above-mentioned charge-transfer interaction, the four-electron destabilizing interaction also contributes to the driving force for the CO_2 bending. As easily seen in Figure 5, the bending of CO_2 decreases two kinds of overlap contributing a four-electron destabilizing interaction, one between Co d_{z^2} and CO_2 $\pi_{\parallel}$ orbitals and the other between Co d_{π} and CO_2 $n\pi_{\parallel}$ orbitals. Such decreases of these overlaps weaken the four-electron destabilizing interaction in the bent structure. The energy decomposition analysis also indicates that the bending of CO_2 reduces destabilization from the EX term, as shown in Table I.

Of the above-described two factors, the decrease in the EX repulsion is about 3 times as large as the increase in the BCTPLX stabilization, suggesting that the weakening of the four-electron destabilizing interaction contributes more to the CO_2 bending than the enhancement of the charge-transfer interaction. In the case of $Ni(PH_3)_2(CO_2)$, the BCTPLX stabilization increases significantly upon the CO_2 bending,[36b] as for $[Co(alcn)_2(CO_2)]^-$. This enhancement of the charge-transfer interaction by the CO_2 bending is explained easily in terms of energy lowering of the CO_2 $\pi^*_{\parallel}$ orbital in this complex as well as in $[Co(alcn)_2(CO_2)]^-$. A difference between $Ni(PH_3)_2(CO_2)$ and $[Co(alcn)_2(CO_2)]^-$ is found in the EX term: in $Ni(PH_3)_2(CO_2)$, the bending of CO_2 has been reported to weaken the EX repulsion to a lesser extent than it strengthens the BCTPLX stabilization.[36b] The Ni d_{π} orbital overlaps little with the p_{π} orbital of the noncoordinating oxygen atom in the η^2 side-on mode (see Figure 4). Therefore, the bending of CO_2 hardly decreases overlap between Ni d_{π} and CO_2 $n\pi_{\parallel}$ orbitals and that between Ni d_{σ} and CO_2 $\pi_{\parallel}$ orbitals. Since the four-electron destabilizing interaction arises from these overlaps, the bending of CO_2 weakens rather slightly the four-electron destabilization in the η^2 side-on mode.

In summary, the driving force for the CO_2 bending is essentially traced to the weakening of the four-electron destabilizing interaction and secondarily to the enhancement of the charge-transfer interaction between Co and CO_2 in the η^1-C mode. In the η^2 side-on mode, the driving force is the enhancement of the charge-transfer interaction supplemented by the weakening of the four-electron destabilizing interaction.

Role of the Coexisting Li^+ Cation in the CO_2 Coordination. In $M[Co(R\text{-}salen)(CO_2)]$, an interaction between the acidic alkali-metal cation and the basic oxygen atom of carbon dioxide has been proposed to play an important role in the CO_2 coordination.[4] To investigate the role of an alkali-metal cation, MO calculations were carried out on $Li[Co(alcn)_2]$ and $Li[Co(alcn)_2(CO_2)]$. Both $Li[Co(R\text{-}salen)]$ and $Li[Co(R\text{-}salen)(CO_2)]$ have been isolated, and the latter has been described as coordinating CO_2 the most strongly among the Li^+, Na^+, and K^+ analogues.[4b] Since the position of Li^+ in $Li[Co(R\text{-}salen)(CO_2)]$ has not been reported, two types of structures were examined:[37] In structure I (Figure 1D), the Li^+ cation is placed at the same position as in the experimental structure of $Li[Co(R\text{-}salen)]$.[4b] In structure II (Figure 1E), the Li^+ cation is equidistant from the two oxygen atoms of the two alcn ligands and from one oxygen atom of carbon dioxide, as found experimentally for the position of K^+ in $K[Co(R\text{-}salen)(CO_2)]$.[4b] In both calculations, the geometry of the $Co(alcn)_2(CO_2)$ moiety was assumed to be the same as in the optimized structure without Li^+.

The binding energy for CO_2 coordination[38a] is calculated to be 5.8 kcal/mol in structure I and 20.0 kcal/mol in structure II,[38b] while moving Li^+ from the position in I to that in II in $Li[Co(alcn)_2]$ causes a very small destabilization of only 2 kcal/mol (see Table II). In spite of a great difference in the binding energies between structures I and II, only small differences are found in the electron populations between these two structures, except for the d_{z^2} orbital population of cobalt (see Table II); the CO_2 coordination decreases the d_{z^2} orbital population by 0.69 e in structure II and by 0.60 e in structure I. Also, the electron population of CO_2 is somewhat larger in structure II than in structure I. These differences found between the two structures suggest that the charge-transfer interaction between Co d_{z^2} and CO_2 $\pi^*_{\parallel}$ is stronger in structure II than in structure I. The weak charge-transfer interaction of structure I is probably due to the fact that in this structure the Li^+ cation would stabilize the cobalt d_{z^2} orbital in energy more than it would the $\pi^*_{\parallel}$ orbital of CO_2 because of its position near Co. In the structure II, since the Li^+ cation is equidistant from CO_2 and $[Co(alcn)_2]$, both the CO_2 π^* and the Co d_{z^2} orbitals become stable in energy to a similar extent. Thus, the Li^+ cation hardly weakens the charge-transfer interaction in structure II but weakens it in structure I, which seems one of the important reasons for the displacement of the Li^+ cation.

The electron population of Li^+ exhibits little change upon the coordination of CO_2 in both structures I and II, as shown in Table III. The energy decomposition analysis of the interaction between the naked Li^+ and CO_2[39] exhibits the importance of ES interaction, EX repulsion, and polarization of CO_2 by Li^+ (Table III). The absence of an effective charge-transfer interaction accords with

(36) (a) In the linear structure, the OCO angle was assumed to be 180°, but the remaining geometrical parameters were taken to be the same as those of the optimized structure of Figure 1A. (b) Going to the bent structure from the linear one, the BCTPLX stabilization increases by 29 kcal/mol but the EX repulsion decreases by 17 kcal/mol. (c) Hoffmann and co-workers have proposed previously that the CX_2 coordination (X = O or S) can be made possible if CX_2 is promoted to an excited state.[14] Their proposal is similar to our explanation given here, since the $\pi^*_{\parallel}$ orbital of CO_2 is populated and CO_2 is bent in the excited state.

(37) Two kinds of K^+ cation, K_1^+ and K_2^+, are found in $K[Co(R\text{-}salen)(CO_2)]$: The K_1^+ cation interacts with carbon dioxide and R-salen (see Figure 1D,E). The K_2^+ cation is surrounded by four oxygen atoms of two carbon dioxides and two oxygen atoms of two R-salen's (see Figure 1 of ref 4b). We have investigated only the former type of alkali-metal cation, which has been described to be more important than the latter.[4b]

(38) (a) The binding energy is defined as follows: $E_i\{Li[Co(alcn)_2(CO_2)]\}_{I \text{ or } II} - E_i\{Li[Co(alcn)_2]^-\}_I - E_i(CO_2)_{eq}$, where the subscripts I and II denote "structure I" and "structure II", respectively. (b) $M[Co(R\text{-}salen)(CO_2)]$ is synthesized in tetrahydrofuran (THF), pyridine (py), or toluene. In the cases of THF and py solutions, the solvation cannot be neglected, which means that the calculated binding energy is overestimated owing to no consideration of solvent. Nevertheless, the effect of Li^+ is considered to be reasonably explained in a qualitative sense, at least. Furthermore, the solvation does not seem important for the CO_2 coordination, since toluene can be used as solvent.

(39) The positions of Li^+ and CO_2 are taken as being the same as in structure II of $Li[Co(alcn)_2(CO_2)]$.

(40) Unfortunately, the energy decomposition analysis for the interaction between $[Co(alcn)_2]^-$ and CO_2 was unsuccessful in the presence of Li^+.

the observation that the Li atomic population hardly changes upon CO_2 coordination in $Li[Co(alcn)_2(CO)_2]$ (see Table II).

In conclusion, the presence of an alkali-metal cation is found to enhance the coordination of carbon dioxide by the electrostatic attractive interaction between Li^+ and CO_2 and the polarization of CO_2 by Li^+.

Acknowledgment. Calculations were carried out with an IBM 3081 instrument at the Centre de Calcul du CNRS in Strasbourg-Cronenbourg, except for some supplemental calculations carried out at the IMS Computer Center with support of a Grant-in-Aid for Scientific Research from the Japanese Ministry of Education, Science, and Culture (No. 60540306). We thank the staffs of the centers for their cooperation. S.S. is grateful to Drs. Benard, Demuynch, and Rohmer for helpful discussions and to the CNRS for financial support.

Registry No. $[Co(alcn)_2(CO_2)]^-$, 108663-10-1.

Contribution from the Christopher Ingold Laboratories, University College London, London, WC1H 0AJ, U.K., and Department of Medical Oncology, The University of Texas M. D. Anderson Hospital and Tumor Institute at Houston, Houston, Texas 77030

Neutral Chain Chloride- and Bromide-Bridged Platinum(II,IV) Complexes of 1,2-Diaminocyclohexane: Synthesis and Electronic, Infrared, Raman, and Resonance Raman Studies

Robin J. H. Clark,*† Vincent B. Croud,† and Abdul R. Khokhar‡

Received February 24, 1987

The synthesis and electronic, infrared, Raman, and resonance Raman spectra of the linear-chain complexes [Pt(*trans*-dach)X_2][Pt(*trans*-dach)X_4] (X = Cl, Br; dach = 1,2-diaminocyclohexane) are reported. The electronic spectra are characterized by broad, intense intervalence bands at ca. 25 000 cm^{-1} for X = Cl and ca. 18 200 cm^{-1} for X = Br. The temperature dependences of the infrared and resonance Raman spectra are discussed with particular reference to the Raman-active ν_1, $\nu_s(X–Pt^{IV}–X)$ mode and the role of unresolved components of this band in determining (a) the dependence on the exciting line of the ν_1 band wavenumber and (b) the excitation profile of ν_1.

Introduction

The complexes under study here, of stoichiometric formula Pt(*trans*-dach)X_3, where X = Cl or Br and dach = 1,2-diaminocyclohexane, were synthesized as part of continuing research into the antitumor activity of dihalo–amine complexes of platinum.[1–4] A X-ray study[5] of Pt(*trans*-dach)Cl_3 has indicated that the structure could be refined equally well in the space group *Pmnm* (centrosymmetric, with a disordered Cl^- above and below the $PtCl_2N_2$ plane) or in $Pmn2_1$ (noncentrosymmetric, 5-coordinate platinum(III)). The present spectroscopic study removes the ambiguity in favor of the former.

Additionally the temperature dependence of the Raman spectra, specifically the exciting-line dependence of the wavenumber of ν_1, $\nu_s(X–Pt^{IV}–X)$, and the form of its excitation profile are discussed in terms of relative intensity changes in unresolved components of ν_1.

Experimental Section

(i) Preparations. Materials. $K_2[PtCl_4]$ was purchased from Johnson Matthey, Seabrook, N.J., and 1,2-diaminocyclohexane, from Aldrich Chemical Co. *trans*-(+)-*S*,*S*-dach and *trans*-(−)-*R*,*R*-dach were purchased from Alfa Thiokol/Ventron Division, Danver, MA 01923.

Methods. Dihalo(1,2-diaminocyclohexane)platinum(II), sulfatoplatinum(II)–water, sulfato(*trans*-(+)-*S*,*S*)-1,2-diaminocyclohexane)-platinum(II)–water, and sulfato(*trans*-(−)-(*R*,*R*)-1,2-diaminocyclohexane)platinum(II)–water were prepared by established methods.[4,6,7]

The (+)-*S*,*S*- and (−)-*R*,*R*-(*trans*-dach)PtX_3 complexes were synthesized by mixing stoichiometric quantities of the appropriate [Pt^{II}(*trans*-dach)(SO_4)] and [Pt^{IV}(*trans*-dach)$(SO_4)X_2$] in water, in the presence of excess of sodium halide.

Pt(*trans*-dach)Cl_3 was synthesized by adding [Pt(*trans*-dach)Cl_2], prepared from a racemic mixture of the trans amine, to concentrated HCl and heating for several hours.

All of the complexes were washed with acetone and diethyl ether and finally dried in vacuo.

Anal. Calcd for [Pt(*trans*-(+)-*S*,*S*-dach)Br_2][Pt(*trans*-(+)-*S*,*S*-dach)Br_4]: C, 13.11; H, 2.55; N, 5.10; Br, 43.71. Found: C, 13.63; H, 2.90; N, 5.25; Br, 42.33. Calcd for [Pt(*trans*-(−)-*R*,*R*-dach)Br_2][Pt(*trans*-(−)-*R*,*R*-dach)Br_4]: C, 13.11; H, 2.55; N, 5.10. Found: C, 13.64; H, 2.26; N, 5.02. Calcd for [Pt(*trans*-(+)-*S*,*S*-dach)Cl_2][Pt(*trans*-(+)-*S*,*S*-dach)Cl_4]: C, 17.32; H, 3.37; N, 6.73. Found: C, 17.53; H, 3.30; N, 6.69. Calcd for [Pt(*trans*-(−)-*R*,*R*-dach)Cl_2][Pt(*trans*-(−)-*R*,*R*-dach)Cl_4]: C, 17.32; H, 3.37; N, 6.73. Found: C, 17.14; H, 3.34; N, 6.45. Calcd for [Pt(dach)Cl_2][Pt(dach)Cl_4]: C, 17.32; H, 3.37; N, 6.73. Found: C, 17.24; H, 3.42; N, 6.61.

(ii) Instrumentation. Electronic spectra were recorded on a Cary 14 spectrometer at 295 K as Nujol mulls of the samples between quartz plates.

Infrared spectra were recorded in the region 650–20 cm^{-1}, as wax disks of the complexes, with a Bruker IFS 113V interferometer. An RIIC liquid-nitrogen cryostat was used to obtain spectra at ca. 80 K.

Raman spectra were recorded on a Spex 14018/R6 spectrometer. (RCA C 31034A photomultiplier). Exciting radiation was provided by Coherent Radiation Model CR 12 and CR 3000 K lasers. Samples were in the form of pressed disks, either of the pure complex or of a mixture with $K_2[SO_4]$. Raman spectra were recorded at ca. 40 K on an Air Products Displex Cryostat and at ca. 80 K with use of liquid nitrogen and a Dewar assembly. The usual technique for determining sample temperatures via Stokes/anti-Stokes ratios is invalid at resonance, and the use of a thermocouple would require that it be placed at the focal point of the laser beam on the crystal surface—a technical impossibility for Raman measurements. Thus, only nominal sample temperatures can be

†University College London.
‡The University of Texas M. D. Anderson Hospital and Tumor Institute at Houston.

(1) Rosenberg, B.; Vancamp, L.; Trosko, J. E.; Mansour, V. H. *Nature (London)* **1969**, *222*, 385.
(2) Gale, G. R.; Walker, E. M.; Atkins, L. M.; Smith, A. B.; Mieschen, S. J. *Res. Commun. Chem. Pathol. Pharmacol.* **1974**, *7*, 529.
(3) Speer, R. J.; Ridgway, H.; Hill, J. H. *Wadley Med. Bull.* **1975**, *5*, 335.
(4) Speer, R. J.; Ridgway, H.; Hill, J. H. *J. Clin. Hematol. Oncol.* **1977**, *7*, 210.
(5) Gebreyes, K.; Zubieta, J. A., unpublished work. The data were collected on a crystal synthesized from the racemic mixture of the trans ligand ca. 0.02 × 0.12 × 0.25 mm at −113 ± 1 °C. The orthorhombic cell parameters, a = 9.312 (2), b = 10.396 (4), and c = 5.698 (3) Å, were refined in space group $Pmn2_1$. The Pt–Pt chain distance ($b/2$) is thus 5.198 Å; cf. that for $[Pt(dach)_2][Pt(dach)_2Cl_2]Cl_4$, which is 5.158 Å: Larsen, K. P.; Toftlund, H. *Acta Chem. Scand., Ser. A*, **1977**, *A31*, 182.
(6) Tobe, M. L.; Khokhar, A. R.; Braddock, B.; Ross, W. C. J.; Jones, M.; Connors, T. A. *Chem.-Biol. Interact.* **1972**, *5*, 415.
(7) Kidani, Y.; Noji, M.; Tsukagoshi, S.; Tashiro, T. *Gann* **1978**, *69*, 263.

0020-1669/87/1326-3284$01.50/0